

Two-layer model of wind-driven circulation in the Antarctic Ocean

Kazuya Kusahara^{1*}, Kay I. Ohshima² and Katsuro Katsumata³

¹Graduate School of Environmental Earth Science, Hokkaido University, Sapporo 060-0810

²Institute of Low Temperature Science, Hokkaido University, Sapporo 060-0819

³School of Geography and Oceanography, University of New South Wales,
Australian Defense Force Academy, Canberra, Australia

(Received March 14, 2003; Accepted August 29, 2003)

Abstract: In this study, we investigate the wind-driven circulation in the Antarctic Ocean using a primitive two-layer model with realistic topography. A prominent feature of steady circulation driven by the annual mean wind stress is a clockwise (cyclonic) circulation in the lower layer at the Weddell Basin and the Australia Antarctic Basin. In particular, the circulation pattern in the Australia Antarctic Basin agrees with the observations. In these basins, negative vorticity input from the wind stress is transmitted to the lower layer through the diffusion term (Gent and McWilliams term) and causes prominent cyclonic gyres within closed geostrophic contours of f/H (f : Coriolis parameter, H : water depth). The model result forced by the seasonal wind stress shows that variations of the Antarctic Coastal Current are explained by wind stress variations along the coast. The transport of this current is determined by the integration of onshore Ekman transport along the coast. It is also shown that this Antarctic Coastal Current can be a part of the western boundary current in the Weddell Sea. On a time scale of 10 to 100 days, the variation of the upper layer thickness coincides with the sea level variation at Syowa Station. This variation might be attributed to coastal trapped waves driven by the alongshore wind stress.

key words: Antarctic Ocean, wind-driven circulation, geostrophic contour

1. Introduction

The Antarctic Ocean is the only ocean that is directly connected with three oceans (the Pacific, Indian and Atlantic Oceans). The formation of Antarctic Bottom Water in the Antarctic Ocean is important for the global ocean circulation and accordingly climate change. The ocean circulation in the Antarctic Ocean is governed by thermohaline and wind-driven dynamics and is strongly modified by the presence of the bottom topography and sea ice. Although many investigations for the Antarctic Circumpolar Current have been discussed by means of both observation and theory, the Antarctic Ocean located south of the Antarctic Circumpolar Current region has not been studied well until now mainly because of observational difficulties.

Gordon *et al.* (1981) proposed that a gyre in the Weddell Sea is wind-driven

*Present address: Institute of Low Temperature Science, Hokkaido University, Kita-19, Nishi-8, Kita-ku, Sapporo 060-0819 (kazu@lowtem.hokudai.ac.jp).

circulation, and they estimated the transport of the western boundary current to be 76 Sv based on the Sverdrup relation. Although there have been several investigations with three dimensional ice-ocean coupled models in the Antarctic Ocean (Häkkinen 1995; Beckmann *et al.*, 1999; Timmermann *et al.*, 2002a, b), all these model studies are simulation-oriented and little dynamical consideration has been paid for the circulation in the Antarctic Ocean.

Though oceanographic data in the Antarctic Ocean are sparse, sea level data at a few stations along the coast of Antarctica are comparatively well maintained. Aoki (2002) found that the sea level variations with the period of 10 to 100 days around the Antarctica are coherent and have significant negative correlation with an index of the atmospheric annular mode variation (the Antarctic Oscillation). He proposed that sea level variations around Antarctica can be explained by the meridional Ekman transport associated with atmospheric variations. Ohshima *et al.* (1996) suggested that the seasonal variations of the thickness of the Winter Water layer off Syowa Station are determined by Ekman convergence along the coast. In their discussion, not only local Ekman convergence but also the convergence in the coastal area far east of the station affect variations of the thickness of Winter Water.

The purpose of this study is to investigate the mechanisms of the wind-driven circulation in the Antarctic Ocean with a two layer model. First, we investigate the steady circulation forced by the annual mean wind stress, with special attention to the clockwise circulation in the lower layer in each basin. Second, we examine the seasonal variation of the Antarctic Coastal Current, reproduced in the model. Finally, we discuss the ocean variation with a period of 10 to 100 days over the coastal areas by comparison with the sea level at Syowa Station.

2. Model

We use a two-layer primitive model in spherical coordinates with the hydrostatic and Boussinesq approximations. The effect of subgrid scale eddies has been incorporated in the model by the diffusion term (GM term) in the continuity equations (Gent and McWilliams, 1990), that is,

$$\frac{\partial \xi}{\partial t} = -\nabla \cdot (H_2 \bar{\mathbf{u}}_2) + \alpha \nabla^2 \xi, \quad (1)$$

where ξ , H_2 , $\bar{\mathbf{u}}_2$ are internal interface displacement, thickness of the lower layer and current vector of the lower layer, respectively. The GM term yields a flow $\alpha \nabla^2 \xi$ across the interface, which stretches or compresses vortex tubes in the lower layer.

Bottom friction is included through a simple linear parameterization. Horizontal friction is modeled as a Laplacian form. Values of the coefficients are shown in Table 1.

The horizontal resolution is 2.25° in the zonal and 1.125° in the meridional direction. The model domain surrounds Antarctica and extends to an artificial boundary at 38°S . The initial thickness of the upper layer is set to 1000 m. Values of other parameters are listed in Table 1.

The objective analysis data of the European Centre for Medium-Range Weather Forecasting (ECMWF) Re-Analysis Data Set have been used for the wind stresses in

Table 1. Values of coefficients and parameters used in the model.

Model type	Realistic model	Idealized model	Unit
Upper layer density	1025	1025	m^3kg^{-1}
Lower layer density	1027	1030	m^3kg^{-1}
Earth radius	6370×10^3	6370×10^3	m
Horizontal viscosity	1.0×10^4	2.0×10^3	m^2s^{-1}
Bottom friction	1.15×10^{-7}	1.15×10^{-7}	s^{-1}
Coefficient of GM (α)	1.75×10^3	4.0×10^3	m^2s^{-1}

this study. Wind stress $\vec{\tau} = (\tau_x, \tau_y)$ is expressed as

$$\tau = \rho_a C_D |\vec{W}_{10}| \vec{W}_{10},$$

where \vec{W}_{10} (ms^{-1}) is the wind vector and ρ_a ($= 1.225 \text{ kg m}^{-3}$) and C_D ($= 1.32 \times 10^{-3}$) are the air density and drag coefficient, respectively. The wind stress data are interpolated linearly to the model grid points (C grid).

The topography data are derived from ETOPO5 (Earth Topography-5 Minute). In order to avoid outcropping of the bottom topography into the top layer, model grids with depth less than 1500 m are assumed to be land.

We use the nonslip boundary condition. To diminish the effect of the northern boundary, a buffer region is placed at the northern 10 grids where the horizontal viscosity exponentially increases 10 times toward the northern edge. The wind stresses north of 50°S decrease linearly to zero at the northern boundary to avoid wave motion at the northern boundary.

3. Results and discussion

The topography in the Antarctic Ocean, shown in Fig. 1, is characterized by three basins: the Weddell Basin, the Australia Antarctic Basin and the Southeast Pacific Basin. Closed geostrophic contours, f/H (f : the Coriolis parameter, H : water depth), are formed there. It should be noted that at these high latitudes the distribution of the geostrophic contours (f/H) are almost identical to that of the depth contours. A region surrounded by geostrophic contours is called a *geostrophic island* by Masuda and Mizuta (1995). Rhines and Young (1982a, b) show that a strong circulation can be formed by only a weak diffusion of vorticity in the geostrophic island.

3.1. Case of annual mean wind stress

Figure 2 shows the annual mean wind stress and the distribution of the wind stress curl. The wind is westward in the coastal area at higher latitude and eastward at lower latitude, yielding negative wind stress curl on the sea surface south of $\sim 50^\circ\text{S}$. In particular, relatively large stress curl can be found off East Antarctica. This annual mean distribution of the wind stress curl indicates that the Antarctic Ocean is a divergence region of Ekman transport and therefore an upwelling region (Webb and Suginohara, 2001).

A quasi steady state is formed after 100-year integration in the experiment with the

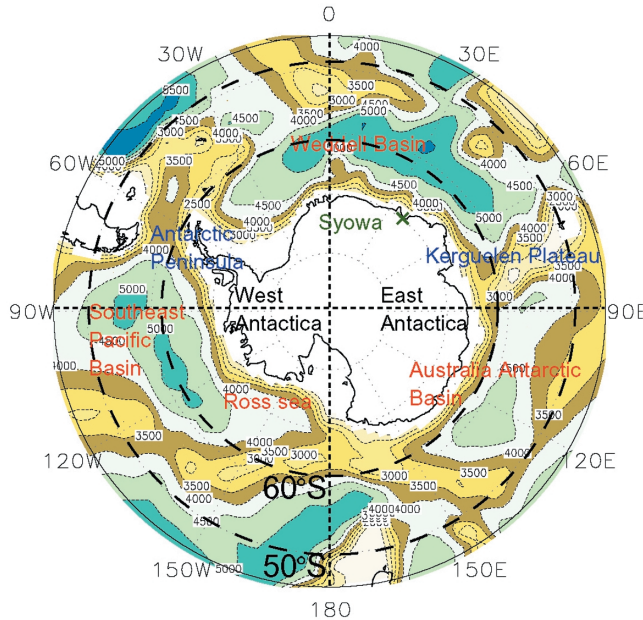


Fig. 1. A bathymetric map of the Antarctic Ocean. The contour interval is 500 m.

annual mean wind stress. The response time can be explained by the transit time of baroclinic Rossby waves across the region (~ 70 years). The coefficient of the GM term influences the spin up time but does not influence the steady flow pattern. Figure 3 shows the velocity fields of the upper and lower layers after 100-year integration. In the upper layer, the Antarctic Circumpolar Current centered around 55°S is reproduced with velocity of about 0.1 m/s. Both in the Weddell Sea and Ross Sea, a cyclonic gyre is formed with a northward flow along the western side, which can be interpreted as a western boundary current. The westward coastal currents are also found as a part of these gyres in the Weddell Sea and the Ross Sea. In the lower layer, the circulation pattern is strongly affected by the bottom topography. Typical flow speed in the lower layer is $\sim 10\%$ of that in the upper layer. In the lower layer, a relatively strong westward flow is formed in coastal regions, and this flow joins the northward flow as a part of the western boundary current in the Weddell Sea. The Antarctic Coastal Current, the westward flow along the Antarctic coast, (Fahrback *et al.*, 1992, 1994) is reproduced well, particularly in the lower layer.

In the Weddell Basin and the Australia Antarctic Basin, low pressure fields are formed with a clockwise circulation. In particular, the circulation patterns in the Australia Antarctic Basin agree well with the flow pattern observed with CTD and ADCP by Donohue *et al.* (1999). On the other hand, in the Southeast Pacific Basin, a clockwise circulation is not formed clearly. These strong clockwise circulations are thought to be a result of the negative vorticity input from the wind stress to the lower layer through the diffusion of the internal interface (that is, GM term) and closed geostrophic contours (Fig. 4 explains this idea.).

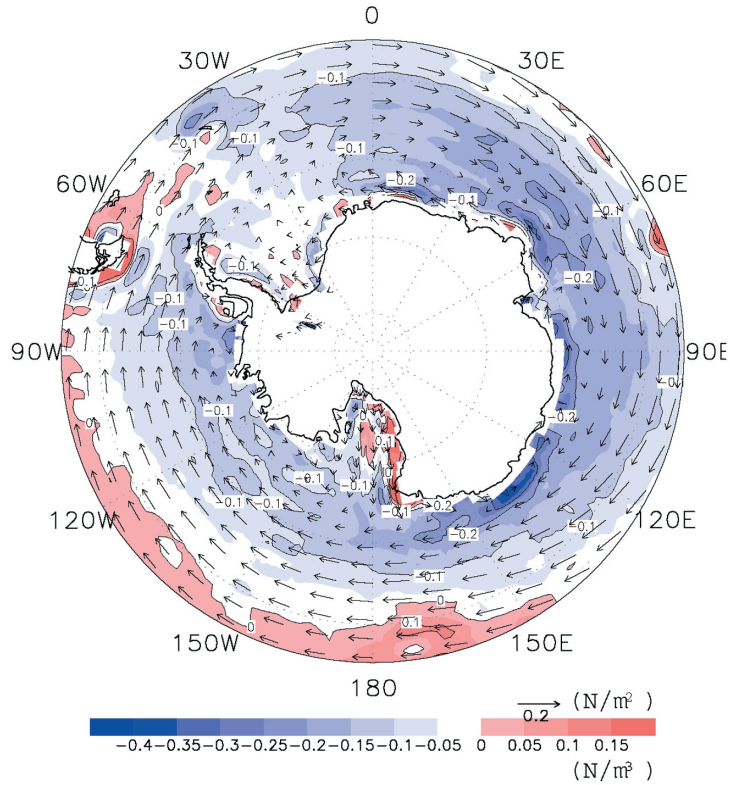


Fig. 2. Annual mean wind stress (vectors, N/m^2) and contours of the associated wind-stress curl (contours, N/m^3) in the Antarctic Ocean, derived from the ECMWF Re-Analysis surface data. The color indicates the strength of the curl.

There are two principal differences between the Southeast Pacific Basin and the other two basins. One is that a geostrophic island is not prominent in the Southeast Pacific Basin. The other is that both positive and negative wind stress curl are found in the Southeast Pacific Basin, while only negative wind stress curl is found in the other two basins. This difference is a result of the difference of the northern extent of the basins; the Southern Pacific Basin extends almost to $40^\circ S$ while the other two extend to about $50^\circ S$ (see Fig. 1 and 2).

3.2. Case of idealized model

Numerical experiments with idealized wind stress and topography were performed to investigate the above two effects on the clockwise circulation: geostrophic island and negative wind stress curl. The horizontal resolution of the idealized model is 1.0° in the zonal direction and 0.4° in the meridional direction. The model domain is the region from 0° to 90° in the zonal direction, from $70^\circ S$ to $30^\circ S$ in the meridional direction. The boundary condition in the idealized model is nonslip and the cyclic condition is applied in the zonal direction. To diminish the effect of the northern and

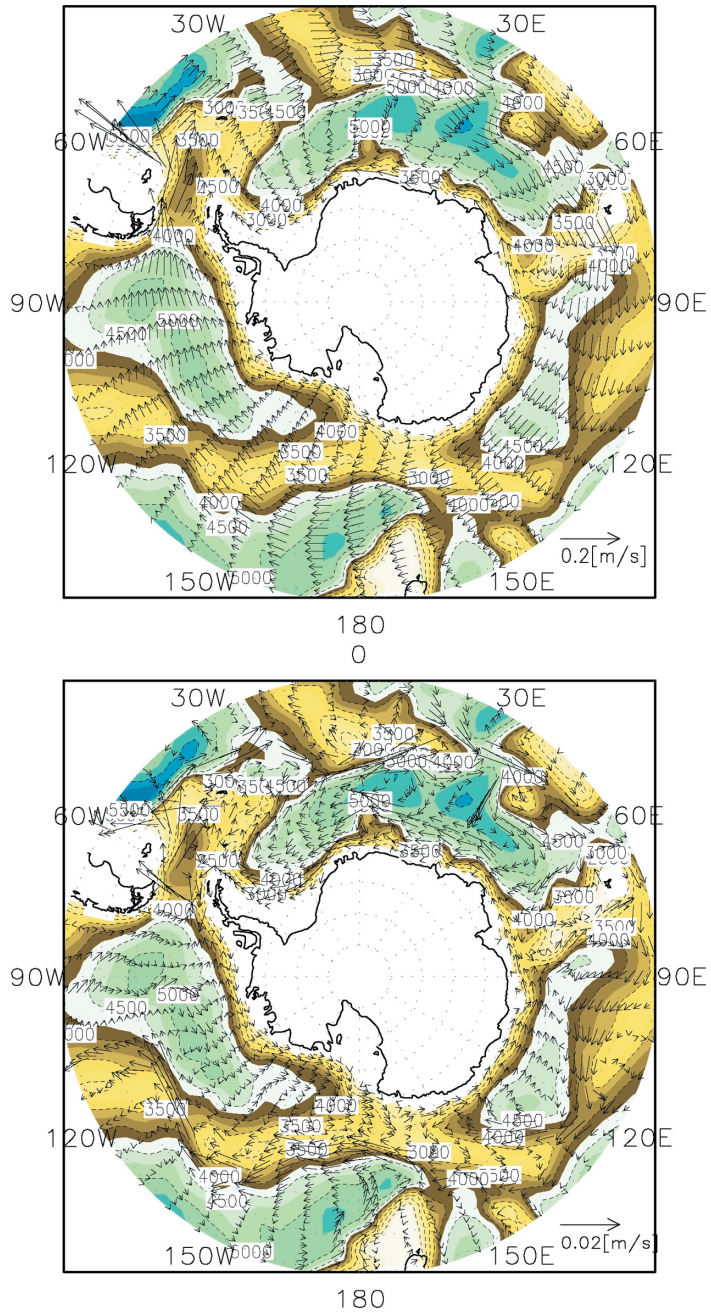


Fig. 3. Results of the steady wind forcing experiment. The upper panel shows the current vectors in the upper layer. The lower panel shows the current vectors in the lower layer. The bathymetric contours are superimposed in both panels.

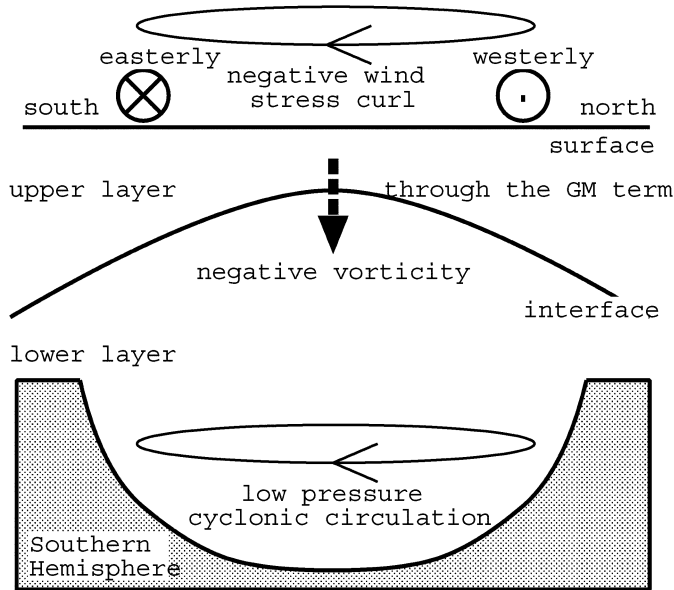


Fig. 4. A schematic diagram of a mechanism for the clockwise circulation in the lower layer.

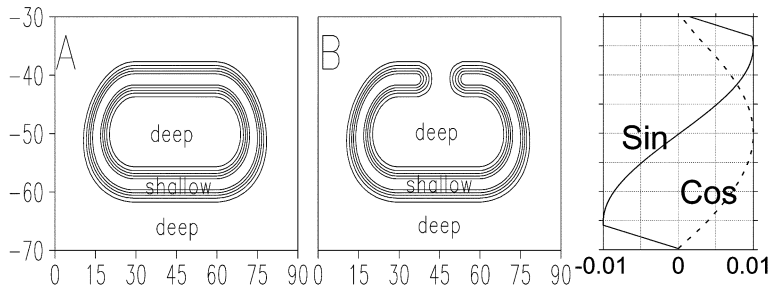


Fig. 5. Geometry (left and middle panels) and wind stress distribution (right panel) in the idealized model. In the left and middle panels, the depth of the deepest region (indicated by “deep”) is 4000 m and the depth of the shallowest region (indicated by “shallow”) is 2500 m. The contour interval is 500 m. Note that the geostrophic contours (f/H) are almost identical to the depth contours. In the right panel, the solid curve indicates “Sin” type wind and the dotted curve indicates “Cos” type wind.

southern boundaries, buffer regions are placed. Figure 5 (left and middle panels) shows the topography of the idealized model. The topography A is a case with a plateau surrounding the basin perfectly. The topography B is the same as A except that the plateau is broken partly. A geostrophic island is formed in A, but not in B. Figure 5 (right panel) shows the two wind stress patterns used in the idealized model. The wind stress is assumed to have only zonal component. Wind “Sin” causes only negative wind stress curl over the basin, while Wind “Cos” causes positive curl over the northern

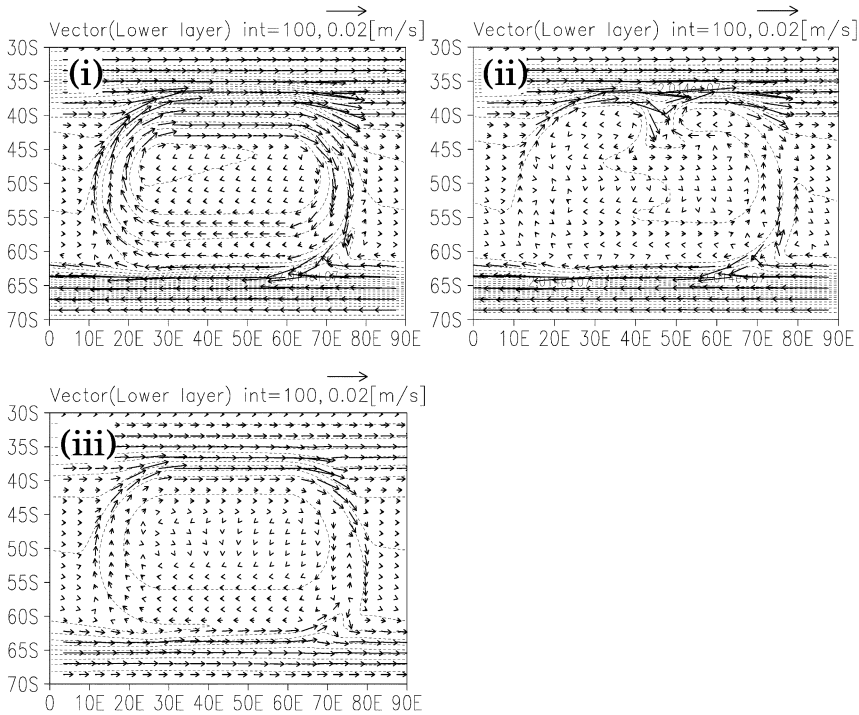


Fig. 6. Pressure and current vectors in the lower layer for cases (i), (ii) and (iii) (see text) in the idealized model. The pressure is indicated by dotted contours.

half of the basin and negative curl over the southern half. Three numerical experiments are performed by using the following topography and wind stress.

- (i) Topography A, and Wind “Sin”.
- (ii) Topography B, and Wind “Sin”.
- (iii) Topography A, and Wind “Cos”.

Figure 6 shows the velocity and pressure fields in the lower layer for these three cases. In case (i), the low pressure field is formed in the basin and a clockwise circulation is exited clearly. In cases (ii) and (iii), a low pressure field is not formed in the basin and a clockwise circulation is not found. From the results of (i) and (ii), the geostrophic island is necessary for forming the low pressure field and the associated clockwise circulation. From the results of (i) and (iii), both positive and negative vorticity from the wind stress compensate for each other and result in almost no circulation. Thus, in the Weddell Basin and the Australia Antarctic Basin, the clockwise circulation is shown to be a result of the closed geographic contours and negative vorticity input from the wind stress to the lower layer through the GM term. In the Southeast Pacific Basin, however, the clockwise circulation is not clear because these two conditions are not well satisfied.

3.3. Case of seasonally varying wind stress

Further 100-year integration with seasonally varying wind stress was performed

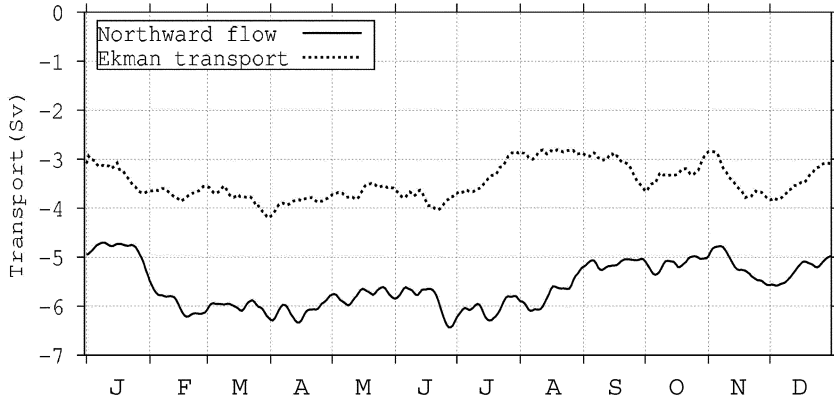


Fig. 7. Seasonal variations of the northward flow in the Weddell Sea (solid line: Negative value indicates northward) and the integrated Ekman transport at coast from 180° westward to the Weddell Sea (dotted line).

from the steady state of the annual mean wind stress. Here, we focus on the seasonal variation of the Antarctic Coastal Current. The westward wind stress along the coast results in Ekman convergence there. It is possible that the wave motion induced by Ekman convergence propagates westward along the coast and becomes part of the northward flow of the western boundary current in the Weddell Basin. From this point of view, the transport of the northward flow in the Weddell Basin (the width of the flow is assumed to be about 200 km from the western boundary) is compared with the integration of meridional Ekman transport at the coast from 180° westward to the Weddell Sea. Figure 7 shows these seasonal variations. The seasonal variation of the integrated Ekman transport (dotted line in Fig. 7) has a maximum of 4.2 Sv in autumn and minimum of ~ 3 Sv from winter to spring, while that of the transport of the northward flow in the Weddell Basin (solid line in Fig. 7) shows a maximum of 6.5 Sv from fall to winter and minimum of 4.7 Sv from spring to summer. The seasonal amplitude is ~ 1.5 Sv for both transports. A lag correlation analysis of the northward flow in the Weddell Basin and the integrated Ekman transport shows a significant maximum of 0.55 with a lag of 9 days, the integrated Ekman transport leading the Weddell transport. The seasonal variation of the northward transport in the Weddell Sea is partly explained by that of the integrated Ekman transport. The steady component of the Ekman transport and northern transport are 3.46 Sv and 5.58 Sv, respectively. We infer that the 62% of steady component of the northward transport is the steady component of the Antarctic Coastal Current driven by the Ekman transport and that the remaining 38% is a western boundary current of the wind-curl driven Weddell gyre.

3.4. Case of daily wind stress

Finally, we examined the relation between the sea level variation at Syowa Station (its location is shown in Fig. 1) and the model result with daily wind stress from 1986 to 1989. Here we focus on the variation with a period of 10 to 100 days. A band pass

filter was applied to both model result and sea level data where the 101-day running mean was subtracted from the 11-day running mean. The result is shown in Fig. 8. The correlation between the sea level variation at Syowa Station and the upper layer thickness in the model is highest (0.42), when no lag is assumed. This indicates that the sea level variation at Syowa Station is related to the variation of the internal interface

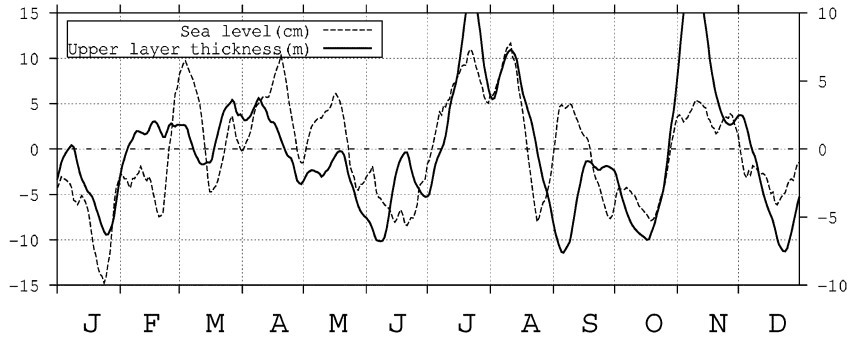


Fig. 8. Time series of the upper layer thickness (solid line) in the experiment forced by the daily ECMWF wind stress and sea level (dotted line) at Syowa Station, Antarctica, in 1988. A band pass filter (extracting 10–100 days variation) was applied to both the upper layer thickness and sea level. The left axis shows the scale for the sea level variation (unit: cm), and the right axis shows the scale for the upper layer thickness variation (unit: m).

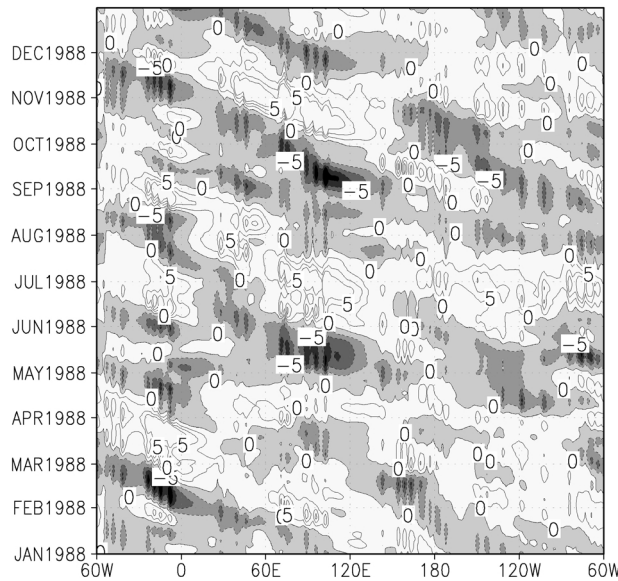


Fig. 9. Time evolution of the anomaly of upper layer thickness along the coast in the experiment forced by the daily wind stress in 1988. Numerals indicate the layer thickness in meters. The shaded areas indicate negative values. The contour interval is 2.5 m.

and is reproduced as the upper layer thickness variation. Figure 9 shows the time evolution of the upper layer thickness along the coast in 1988. The anomalies of the upper layer thickness propagate westward with the coast on the left hand side. This propagation has wavenumber 2 with the phase speed being about 1.63 (m/s). The discontinuities near 65°W and 170°E are thought to be a result of the western boundaries of the Weddell Sea and the Ross Sea. The phase speed of internal Kelvin wave in a two layer model is

$$c_{\text{ideal}} = \sqrt{g \frac{(\rho_2 - \rho_1)}{\rho_2} \frac{H_1 H_2}{(H_1 + H_2)}}$$

(Gill, 1982). Typical parameters in the coastal area of this model, ($H_1 = 200$ m and $H_2 = 1800$ m) give $c_{\text{ideal}} = 1.85$ (m/s), which is within 15% of the model result.

This model can not resolve the internal deformation radius of 14 km. Anderson *et al.* (1979) showed that the internal Kelvin wave like motions are reproduced to some extent even in a coarse resolution model with the phase speed being somewhat slower. This might explain why the propagation speed in the model (1.63 m/s) is slower than the ideal phase speed of the internal Kelvin wave (1.85 m/s).

4. Conclusions

The purpose of this study is to investigate the mechanisms of wind-driven circulation in the Antarctic Ocean with a two-layer model. The topography in the Antarctic Ocean is characterized by three basins: the Weddell Basin, the Australia Antarctic Basin, and the Southeast Pacific Basin. The wind blows westward in the coastal area at higher latitude and eastward at lower latitude. Negative wind stress curl acts on the sea surface south of ~50°S.

First, we investigate the steady state forced by the annual mean wind stress. In the upper layer, the Antarctic Circumpolar Current centered at 55°S is reproduced. In the Weddell Sea and Ross Sea, cyclonic gyres are formed with western boundary currents. The circulation pattern in the lower layer is strongly affected by the bottom topography. In the Weddell Basin and Australia Antarctic Basin, the low pressure field is formed with a clockwise circulation. In particular, the circulation pattern in the Australia Antarctic Basin agrees well with the schematic flow pattern represented from the observations (CTD, ADCP) by Donohue *et al.* (1999). These distinct clockwise circulations are shown to be a result of closed geostrophic contours and negative vorticity input from the wind stress to the lower layer through the GM term (Fig. 4). In the Southeast Pacific Basin, the clockwise (cyclonic) circulation is not clear because the both conditions are not well satisfied.

Second, the model is driven by a seasonally varying wind stress. Seasonal variation of the integrated Ekman transport along the coast coincides with the variation of the northward flow near the coast in the Weddell Sea. The amplitudes of these seasonal variations are comparable. The transport of the Antarctic Coastal Current is determined by the integrated Ekman transport along the coast and can be a part of the western boundary current of the Weddell Sea.

Finally, the model is driven by the daily (1986–1989) wind stress. On time scale of

10 to 100 days, the correlation between the sea level variation at Syowa Station and the upper layer thickness in the model is significant and highest when no lag is assumed. It is shown that the anomaly of the upper layer thickness over the coast propagates westward with the coast on the left hand side. The sea level variation observed at Syowa Station might be partly explained by coastal trapped waves driven by the alongshore wind stress.

Acknowledgments

We are much indebted to Dr. M. Wakatsuchi, A. Kubokawa and G. Mizuta or their valuable comments. Thanks are extended to Takayoshi Ikeda for correcting the manuscript.

References

- Anderson, D.L., Bryan, K., Gill A.E. and Pacanowski R.C. (1979): The transient response of the North Atlantic: Some model studies. *J. Geophys. Res.*, **84**, 4795–4815.
- Aoki, S. (2002): Coherent sea level response to the Antarctic Oscillation. *Geophys. Res. Lett.*, **29**, No. 20, 1950, doi: 10.1029/2002GL015733.
- Beckmann, A., Hellmer H.H. and Timmermann, R. (1999): A numerical model of the Weddell Sea: Large-scale circulation and water mass distribution. *J. Geophys. Res.*, **104**, 23375–23391.
- Donohue, K.A. (1999): Sources and transport of the Deep Western Boundary Current east of the Kerguelen Plateau. *Geophys. Res. Lett.*, **26**, 851–854.
- Fahrbach, E., Rohardt, G. and Krause, G. (1992): The Antarctic Coastal Current in the southeastern Weddell Sea. *Polar Biol.*, **12**, 171–182.
- Fahrbach, E., Rohardt, G., Schröder, M. and Strass, V. (1994): Transport and structure of the Weddell Gyre. *Ann. Geophys.*, **12**, 840–855.
- Gent, P.R. and McWilliams, J.C. (1990): Isopycnal Mixing in Ocean Circulation Models. *J. Phys. Oceanogr.*, **20**, 150–155.
- Gill, A.E. (1982): *Atmosphere-Ocean Dynamics*. New York, Academic Press, 662 p.
- Gordon, A.L., Martinson, D.G. and Taylor, H.W. (1981): The wind-driven circulation in the Weddell-Enderby Basin. *Deep-Sea Res.*, **28**, 151–163.
- Häkkinen, S. (1995): Seasonal simulation of the Southern Ocean coupled ice-ocean system. *J. Geophys. Res.*, **100**, 22733–22748.
- Masuda, A. and Mizuta, G. (1995): A study on the effects of bottom topography on deep circulation with a diffusive reduced-gravity model. *J. Phys. Oceanogr.*, **25**, 374–390.
- Ohshima, K.I., Takizawa, T., Ushio, S. and Kawamura, T. (1996): Seasonal variations of the Antarctic coastal ocean in the vicinity of Lützow-Holm Bay. *J. Geophys. Res.*, **101**, 20617–20628.
- Rhines, P.B. and Young, W.R. (1982a): Homogenization of potential vorticity in planetary gyres. *J. Fluid Mech.*, **102**, 347–367.
- Rhines, P.B. and Young, W.R. (1982b): A theory of wind-driven circulation. I. Mid-ocean gyres. *J. Mar. Res.*, **40** suppl., 559–596.
- Timmermann, R., Beckmann, A. and Hellmer, H. (2002a): Simulations of ice-ocean dynamics in the Weddell Sea 1. Model configuration and validation. *J. Geophys. Res.*, **107**, No. C3, 10.1029/2000JC000741.
- Timmermann, R., Hellmer, H. and Beckmann, A. (2002b): Simulations of ice-ocean dynamics in the Weddell Sea 2. Interannual variability 1985-1993. *J. Geophys. Res.*, **107**, No. C3, 10.1029/2000JC000742.
- Webb, D.J. and Suginohara, N. (2001): Vertical mixing in the ocean. *Nature.*, **409**, 37.